7th Asia-Pacific Workshop on Structural Health Monitoring
November 12-15, 2018 Hong Kong SAR, P.R. China

Performance of Rayleigh based Distributed Optical Fiber Sensors bonded to reinforcing bars in bending

M.F. Bado [1]*, J. R. Casas [2], A. S. Barrias [2]

[1] Institute of Building and Bridge Structures, Vilnius Gediminas Technical University, Vilnius, Lithuania
Email: mattia_francesco@hotmail.com

[2] Institute of Civil and Environmental Engineering, Universidad Politécnica de Cataluña, Barcelona, Spain
Email: joan.ramon.casas@upc.edu; antonio.jose.de.sousa@upc.edu

KEYWORDS: Distributed Optical Fiber Sensors; Structural Health Monitoring; Bending test; Strain Reading Anomalies; Disruption Mechanisms

ABSTRACT

Distributed Optical Fiber Sensors (DOFS) are optimal tools for mapping temperature, strain and vibration inside a structural element in two or even three dimensions. Thanks to their multiple sensing points, wide location range monitoring and customizable spatial resolution, the DOFS allow to paint a clear picture of the global behavior of a structure rather than reporting the tensile state of a limited number of points. This makes it ideal for the detection of deformations and cracking in reinforced concrete (RC) structures, crucial as a mean to ensure the safety of the infrastructure by identifying early signs of excessive damage and giving feedback on the structure's ability to continue serving its intended purpose[1]. Yet, one of the main points holding back such technique are unexplained rise of anomalies in its readings beyond a certain point of any experimental test. Indeed, during multiple DOFS-monitored structural tests (Rayleigh scattering based), researchers have come across strain reading anomalies in the form of excessively large strain peaks with no physical meaning and veracity. The present paper outlines the results obtained by an experimental test developed in the UPC´s Structure Technology Laboratory with the goal of inducing such anomalies under different conditions in order to isolate and identify the cause of their origin. The test consists in gradually bending seven steel reinforcement bars with a DOFS bonded to their bottom tensile surface. The DOFS performance is then studied for different bonding conditions (different adhesives and their layering for every bar), for constant versus varying re-bar sections (some incisions were performed in the rebars) and for different loading speeds (slow, fast and impact). In this paper important conclusions are developed which shed light on such phenomena and lay the grounds for an entirely anomaly-free DOFS-monitored test on RC ties planned as follow-up test.

1. Introduction

Structural Health Monitoring (SHM) techniques are finalized to the detection of deformation and cracking in concrete structures as a mean to ensure the safety of the infrastructure by identifying early signs of excessive damage and giving feedback on the structure's ability to continue serving its intended purpose. Henceforth it crucially helps preventing the adverse social, economic, ecological, and aesthetic impacts that may occur in the case of structural deficiency. In the modern age the most commonly used

* Corresponding author.

tools for capturing information on the structure's health and efficiency are electrical strain sensors, accelerometers, inclinometers, GPS based sensors, acoustic emission, wave propagation, etc. Yet, these methods have serious deficiencies among which the most significant are their sensibility insufficient sensitivity to damage of applied methods, or to environmental disturbances[2]. More sophisticated optical fiber sensing technique such as Fiber Bragg Grating (FBG) sensors[3] also have evident shortcomings among which the limited strain location range monitoring. These shortcomings prevent the possibility of precisely pointing out the location where the damage first occurs and prevents the linking of local damage mechanisms to the global condition of the structure[4]. This limitation is surpassed by Distributed Optic Fiber Sensors (DOFS). The fundamental principle of DOFS is the ability to measure strain and/or temperature along the fiber's length by means of light scattering whenever the photons of the emitted light interacts with physical medium where this occurs (the fiber itself) and its with local material characteristic features like density, temperature and strain[5]. Three different types of scattering processes may occur in a DOF sensor, Raman, Brillouin and Rayleigh scattering but all hold particular optical features that make one more suitable than others relatively to the research objectives. The scattering phenomenon considered in the current paper is the Rayleigh scattering. Despite its 70m sensing range limit, it can provide a high spatial resolution (up to 1 mm), which is ideal for strain and damage monitoring in concrete structures. The latter is often used in experimental laboratory investigations having the DOFS bonded either to its surface, in order to monitor its strains and damages [6-7] and/or on the reinforcement bars that will later be embedded in the concrete [9-11].
The distributed nature of such fibers enables the mapping of temperature, strain and vibration distributions in two or even three dimensions and their identification at any point along a fiber, henceforth allowing the painting of a clear picture of the global behavior of a structure rather than reporting the tensile state of a limited number of points[8]. This, in addition to its high accuracy, long-term stability, durability, and insensitivity to electromagnetic influences, corrosion, and humidity represents the great potential of the DOFS technique. Despite such, at the present moment the technique is still undergoing studying and research and therefore hasn't been standardized yet nor there are clear guidelines on how to ensure every deployment's success.

2. Experimental application of the Distributed Optical Fiber Sensors

2.1 Test motivation

One of the main points holding back such technique from becoming a truly universal and trust-worthy strain reading method is the understanding of the anomalies phenomena which, whenever spring up, compromises the successful measurement of the tensile state of the fiber's support. Multiple publications based on DOFS-monitored experimental campaigns report coming across strain reading anomalies (SRAs) in the form of localized and excessively large strain peaks[9-12] which seemingly have little to no physical meaning or explanation. In some occasions the DOFS may even report that in a specific section of the supporting structure a slight increase in load causes a large tensile strain (peak in the tensile area) followed by an equally large compressive strain (peak in the compressive area). This situation occurs also in the experimental test described in this paper as shown in (Fig. 3) and (Fig. 6). The phenomena here described has little to no physical meaning, suggesting that it might simply be an erroneous DOFS strain reading. This assumption is confirmed when comparing the DOFS's measured strain profile with theoretical models and simultaneous strain gauges monitoring. In both cases, there is no agreement with the DOFS's reported strain peaks suggesting that these are in fact SRAs. Additionally, in papers [9] [12] such anomalies seem to spring up soon after the appearance of the first concrete damage sign suggesting that there might be a connection between the two.

SRAs should obviously be avoided as they prevent the possibility of getting reliable measurements in the single location of the anomalies (time-wise and geometrical-wise anomalies) and extensively increase the level of unreliability of the surrounding measurements. The present paper discusses the results of an experimental investigation campaign designed to shed light on such phenomena and extrapolate some directives on how to run an anomaly-free DOFS-monitored experimental campaign.

This will finally allow researchers to fully embrace the DOFS monitoring technique without concerns of measurement unreliability.

2.2 Test specimen and experimental setup

The authors have conceived an experimental test aimed at pin-pointing the motive behind the rise of SRAs. The test intends on inducing these in a controlled environment under different conditions in order to isolate and identify the cause of their origin. As visible in (Fig. 1), the experiment, carried out in UPC-BarcelonaTech's laboratory, saw the loading of seven parallel Ø20 S500 steel reinforcement bars with their extremities welded to two C shaped steel beams (herein the assumption of a fixed beam behavior). Six of the rebars were instrumented with a single 5 meters long DOFS while one was instrumented with strain gauges for comparison purposes. All were bonded to the lower face of the bars. The research used an Optical Distributed Sensor Interrogator (ODiSI-A) manufactured by LUNA which analyzed the Rayleigh backscatter from a standard single-mode DOFS set to measure strains and temperature.

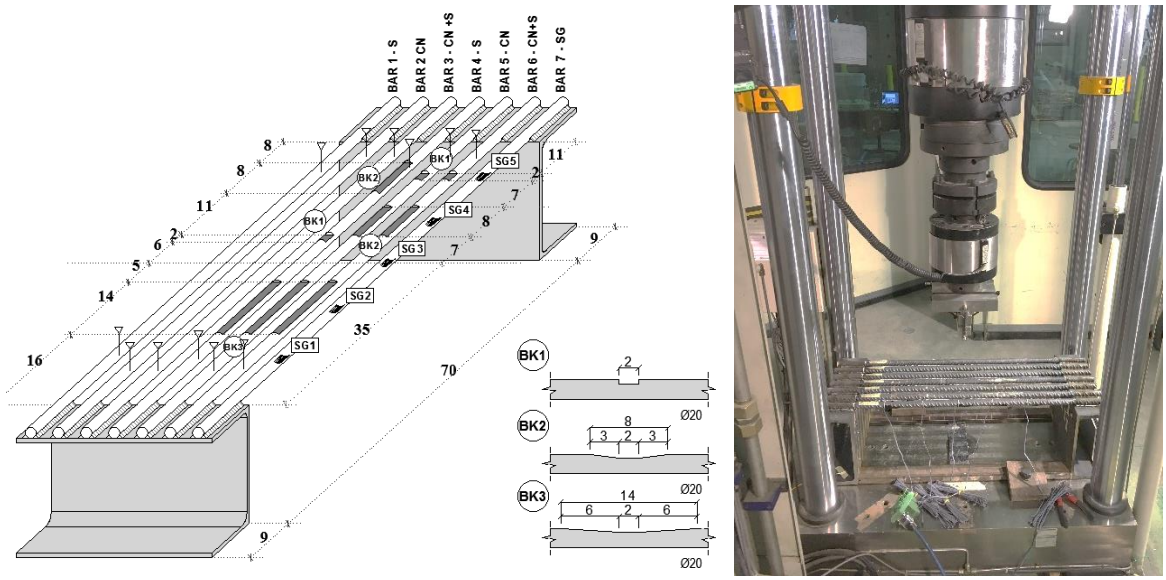

Figure 1. (a) Specimen detailing (b) Test setup with the specimen positioned below the INSTRON hydraulic actuator

The test surveyed the DOFS performance for different bonding conditions, re-bar sections and loading speed. Indeed, two kinds of adhesives were used in order to bond the DOFS to the bars. Cyanoacrylate for Bar 2 and Bar 5; silicone for Bar 3 and Bar 6; cyanoacrylate with an extra silicone layer on top for Bar 1 and Bar 4. Furthermore, Bars 4, 5, 6 were incised along their upper face in order to locally reduce their sectional area. The dimension of such incisions can be read in (Fig. 1). As seen there, some incisions are very sharply-edged (BK1) meanwhile others appear smoother (BK2 and BK3). The bars were loaded simultaneously in their mid-span with different speeds and with two impact loads. As mentioned above the test was designed to study multiple scenarios that cause the strain reading failure SRAs. These scenarios will henceforth be called Disruption Mechanisms (DM) and below are listed seven of these, each followed by the experiment's attempt at simulating them.

(DM-SB1) The excessive bending of the bar (the fiber's support) beyond a certain point may be too high for tensile and shear strength of the fiber's constituting material resistance therefore causing SRAs in the produced readings. The existence of such strain value beyond which anomalies are consistently more susceptible to be triggered is herein defined as Anomalistic strain threshold (AST). The veracity/influence of such disruption mechanism will be examined by applying an increasingly larger bending load on the rebars while constantly monitoring the strains on the lookout for the appearance of SRAs.

(DM-SB2) When the first crack appears in a bending RC member, the stress in the tensile rebar in the cracked section increases exponentially as the steel suddenly passes from simply contributing to resisting the local tensile stress concurrently with the concrete to bearing alone the whole tensile stress (having the concrete cracked). The abrupt peaking of stresses in the steel rebar will automatically lead to a larger strain in the latter (even 20 times bigger than its previous value). Logically, the bonded DOFS will suffer from the same sudden increase in stresses and strains potentially leading to the disruption of the reading capacity of the fiber. In order to simulate such, two impact loads are applied on the bars during the test. If the fiber is able to deliver reliable readings after suffering the impact loads, then it can be assumed that DM-SB2 doesn't affect the DOFS's performance. It should be noted that the sudden increase in stresses in the rebar when a bending RC member cracks is very large and could not be simulated in the present test as it would lead to an excessive sudden bending of the bars and DOFS. Because of such the impact loads were limited to 0.1kN and 1.0kN causing in each bar an increase of respectively 1.6MPa and 16.0MPa.

(DM-SB3) According to the stress-transfer approach[13], the sections of a RC member whose concrete has cracked present a peaking of stresses in the rebar while the tensile state of the sections distant from the cracks remain mostly unaltered. This is due to stresses being transferred from concrete to steel the closer the case-study section is to the cracked section. How quickly such stresses are transferred is a function of the transmission length l_t. An excessively quick transfer of stresses from concrete to steel (corresponding to a short l_t on either side of the cracked section) could be the cause of errors in the DOFS readings. In order to simulate different transmission lengths, three experimented rebars presented incisions with steep or inclined/smooth edges. The reduced area of the rebars leads to increased carried stresses in the incised sections, similarly to what happens in RC member sections that have cracked compared to those that haven't. A steep edge of the incision (Block 1) can be compared to a short transmission length l_t while a sloping one (Block 2, 3) can be compared to a long l_t. The strains in these three rebars are closely monitored in order to verify whether a drastic section variation gradient (Block 1) could cause SRAs and if so earlier than softer-edged incisions.

(DM-AD1) Taking in consideration a RC member with DOFS-instrumented rebars, if the adhesive positioned on top of the fiber isn't protective enough (not thick enough or composed of excessively deformable material), then the cracking concrete friction against the fiber may cause alterations in it leading to SRAs. While DM-AD1 couldn't have been checked with the present test, being it deprived of concrete, it was nonetheless possible to check the difference in the strain reading capacity of the DOFS when it was covered by a double layer of adhesive (having respectively a bonding and protective function). This is the reason why cyanoacrylate with an extra silicone layer on top were deployed in bars 1 and 4.

(DM-AD2) To a certain extent, being completely embedded in adhesive, the DOFS reports the latter's strains and not the supporting structure's. Under the hypothesis of perfect bond between adhesive and supporting structure the strains are identical but this may not always be true. When adhesives harden, they deliver their top stiffness performance ensuring the strongest bond with the structural element but they may also acquire deformative features (fragility, segmented behavior, etc.) that could lead, when under stress, to their delamination and cracking altering the performance of the embedded fiber. During the loading phase the adhesives were monitored in order to spot eventual deterioration.

(DM-AD3) An incorrect DOFS confinement design may lead to altered strain readings. The use of an adhesive with poor confining strength properties or the application of an insufficiently thick layer may cause the fiber to delaminate from its support, therefore losing the hypothesis of perfect bond with its support. Similarly, to before, the adhesives were monitored during the test in order to spot any delamination.

(DM-AD4) It is possible that the viscosity of the adhesive (significant when using silicone) influences the fiber's performance ensuring a minimum amount of slip between the fiber and the adhesive. This allows in consequence a major stress redistribution along the sections in the vicinity, that could be detrimental to the strain readings if a high level of precision is required but could be the key in avoiding premature SRAs. The readings of the portion of the DOFS being bonded with cyanoacrylate was compared to that coming from the portion bonded with silicone.

2.3 Test procedure and outputs

During the test, the specimen was subjected to two loading speeds and two impact loads. At 880 and 1835 seconds two impact loads (0.1 and 1.0 kN respectively) were applied followed by a 60 seconds hold. Before the second impact load (1835 secs) the loading speed was set at 0.35 kN/min while after at 1.12 kN/min until the specimen's plasticity was reached (Fig. 2).

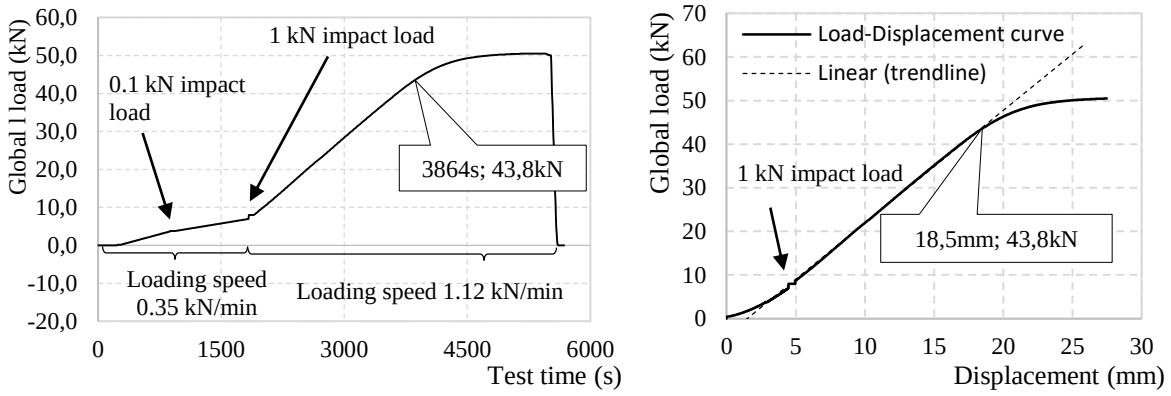

Figure 2. Test load curve over (a) Time and (b) Deflection as measured from the INSTRON Hydraulic Actuator

The different outputs of the DOFS measurements are herein presented. (Fig. 3) represents the DOFS global strain diagram along the whole 5,21m long fiber at three specific instances and increasing load levels. (Fig. 4) instead expands on the previous graph by adding an extra dimension, time. It is therefore possible to visualize in one graph the strain evolution of all six bars, including the appearance of SRAs. In both graphs, the strain profiles of the six DOFS-instrumented bars are represented by the six peaks while the sections of the fiber reporting deformation equals to 0με are those that aren't bonded to any surface and act as simple connections between the glued sections. On both sides of each tensile peak are compressive measurements that do not represent the entirety of the compressive strain profile of the bars as the DOFS wasn't glued all the way to the supports of the bars. If to consider, instead, the strain profile at 3889 seconds and at an applied global load of 43,82kN some SRAs are visible (mid-span of Bar 2 and Bar 3) making the strain readings impossible in those anomalistic areas. Furthermore, the strain profile's loss of linearity in the segment corresponding to Bars 4, 5, 6 is congruous with the rebars' sections that have been incised making them easily recognizable on the measured DOFS strain profile. Before and after the incision's variation in the profile, the linearity is re-acquired. This essentially demonstrates the DOFS ability to read strains free of SRAs despite the presence of incisions with and without steep edges therefore discarding (DM-SB2) as a possible disruption mechanism.

If to compare the strain profile of all the seven rebars at 3089 seconds and a global load of 30.0kN (Fig. 5) (the similarity among them is evident (except for the local increase in strain in the location of the incisions) along with their correspondence with the strain gauges' measurements. Strain gauge 2 seems to be the only one not reporting correct values, probably due to a slight damage suffered during the gluing process. This embodies one more advantage of the DOFS; differently than the strain gauges, the latter doesn´t require fixing at every sensing point, making so that the correct positioning of the fiber is enough to ensure the reading capacity and reliability of each point. The comparison among each bar's DOFS strain profile along with their coherence with the strain gauges' measurements is a testament to the performance and the reliability of the DOFS as a strain sensing technique.

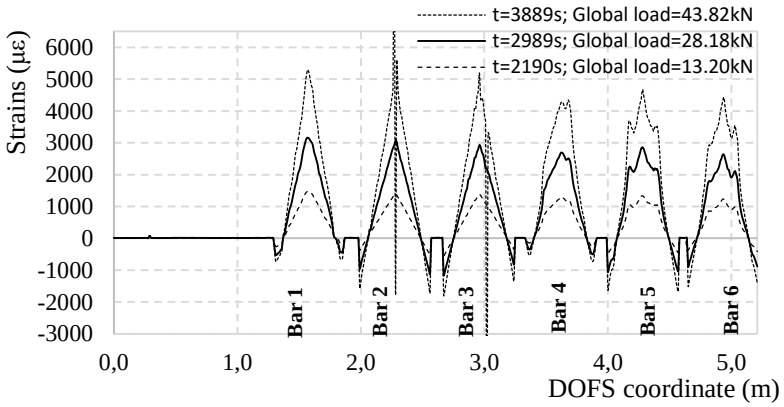

Figure 3. DOFS strain profiles at specific time and global load instances along the test

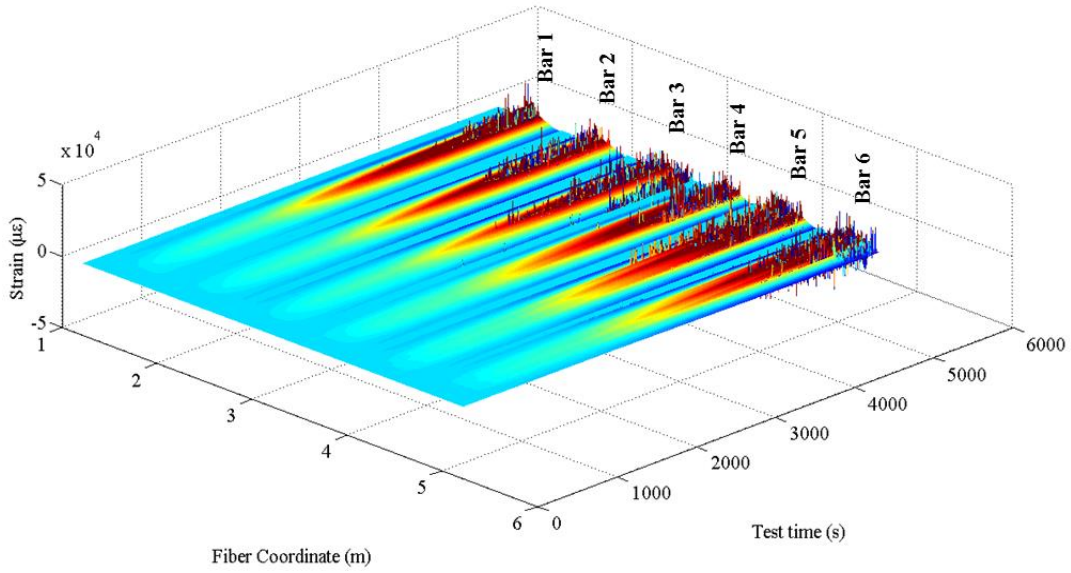

Figure 4. Three dimensional representation of the strains measured by the DOFS over time along the fiber

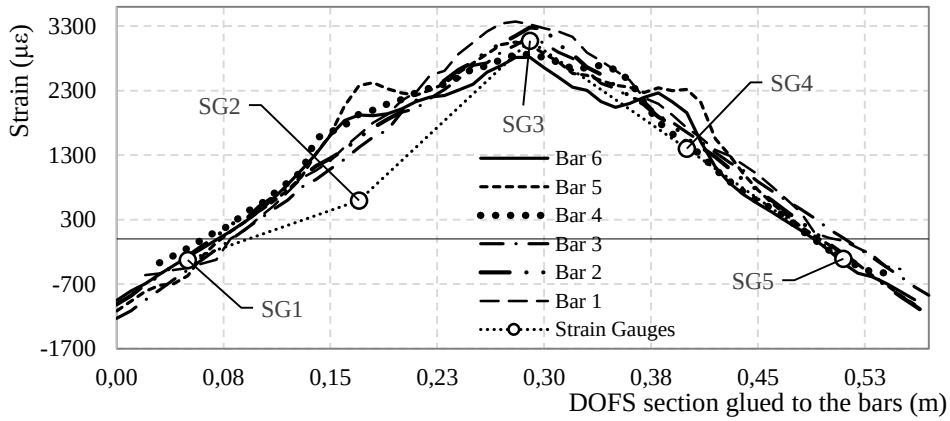

Figure 5. Comparison between the different DOFS-measured strain profile segments bonded to each rebar and by the strain gauges for a global load value of 30.0kN

Below, (Fig. 6) represents the measured strain in six points of the fiber corresponding to the mid-spans of the six bars from the first moment the bars were loaded (point O) until the end of the test including the instances at which the impact loads were applied (I_1 and I_2). After around 3800s (Point B) the profiles are completely dominated by SRAs making it impossible to extract any reliable strain values.

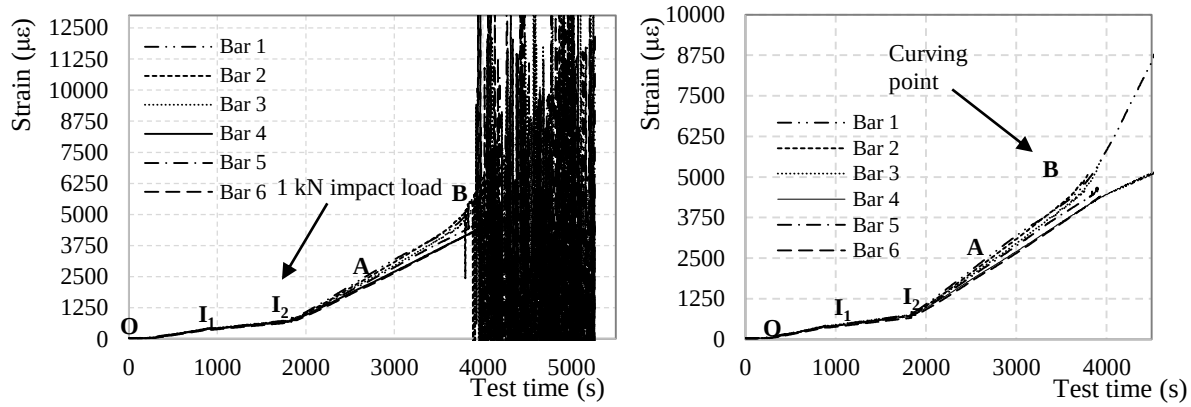

Figure 6. (a) The DOFS-measured strains of the mid-span of every bar along time (b) DOFS-measured strains of the mid-span of every bar along time after erasing the SRAs

3. Discussion of the experimental results and studying of the anomalistic phenomena

In order to comprehensively study the anomalies rising in the DOFS strain readings it is essential to analytically define what is an SRA. The authors suggest here a novel way of identifying them. Given that, by definition of SRA, they correspond to geometrical discontinuities of the Strains/Time or Strains/DOFS coordinate diagrams it is sufficient to set a specific value of strain increment that, when compared to the difference of strain values between two consecutive measurements, if surpassed it indicates the presence of an anomaly. In the present research such value was set to be 200με. The scale of the SRAs and of such strain limit can be seen in (Fig. 7).

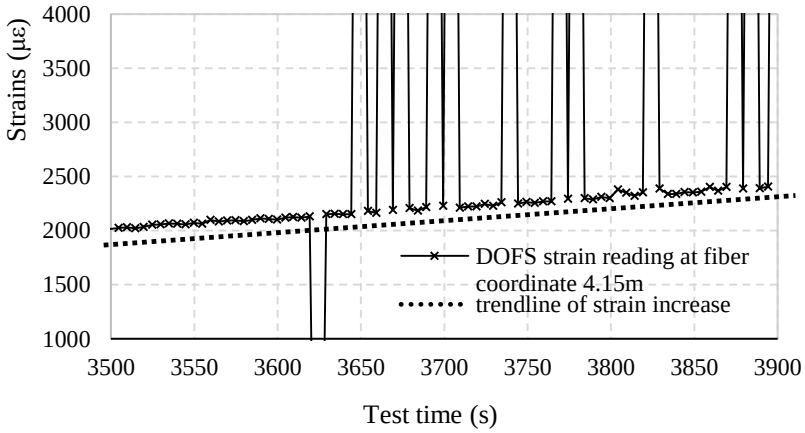

Figure 7. DOFS-measured strains of fiber coordinate 4.15m along time

With this in mind several considerations can be developed on the test outputs of (Fig. 6) that will help defining the anomalistic phenomena:

- The strain profiles until point B are clear and SRA-free. Point B seems to correspond to a strain value of 4000με.
- The strain profiles correspond well with the applied load. The reason behind the difference among the bar's strain profiles is is the lack of perfect planarity of the top surface of the

specimen. Obviously some rebars are slightly higher than others therefore being loaded first and to a higher extent.

- The strain profiles report correctly and precisely the strain variation due to the varying loading speed and are clear even beyond the yielding of the steel rebars (around 2500με for S500 steel marked as point A in (Fig. 6).
- All the segments of the DOFS have successfully recorded both impact loads demonstrating their ability to correctly withstand and record a sudden stress increase of 1.6MPa and 16.0MPa.
- As visible in the strain profiles represented in (Fig. 6b), which have been cleaned of SRAs, the different bars seem to start curving at point B which is in agreement with (Fig. 2).

It should be noted that here, also in agreement with (Fig. 2), the strain profiles don't report a change of linearity beyond the steel yielding strain, due to the fact that the bars aren't loaded uniformly and therefore yield at successive instances. As a matter of fact, the load-displacement curve doesn't deviate from its linear trend until the extremities of all bars haven't yielded. Only once the last of the six bars acquires plastic hinges (both sides of Bar 4 yield at 3864 seconds), the load/displacement and load/strain diagrams begin to clearly deviate from linearity. This point will henceforth be called Plasticity point (represented point B). Coincidentally, the SRAs seem to spring up at this instance suggesting that a loss in linearity in the specimen's load-displacement curve, could be what triggers the SRAs. On the other hand, the anomalies seem to be activated in the proximity of a specific value (around 4000με) that would embody in the present case the anomalistic strain value AST as suggested by (DM-SB1).

However, the anomalistic analysis should not only be run in the mid-span of the rebars, as in (Fig. 6), but on its entire length. Indeed, SRAs don't only rise there and in addition do not necessarily rise there in the first place. (Fig. 4) and (Fig. 8) are a 3-dimensional and 2-dimensional graph representing the DOFS-measured-strains in the six bars versus the test time. In (Fig. 4) the SRAs can be identified as perpendicular peaks whilst in (Fig. 8) they can be identified as black bars. Such graphs allow to not only locate the SRAs in time but also geometrically allowing them to be correlated with the section of the rebars. (Fig. 9) zooms in (Fig. 8) to focus strictly on Bar 5 and reports the strain values at which the SRAs occur.

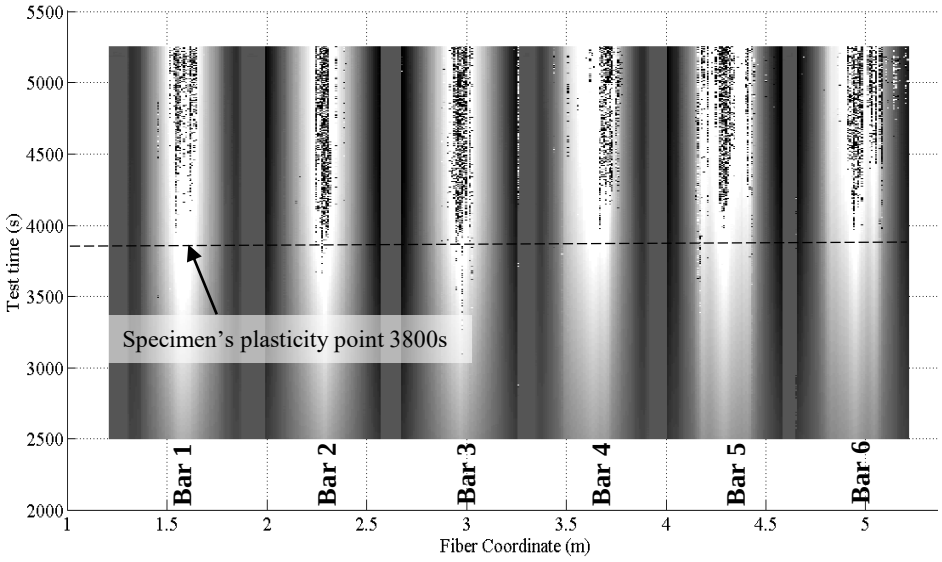

Figure 8. Two dimensional representation of DOFS-measured strains along time over the whole span of the fiber bonded to the rebars and of the SRAs

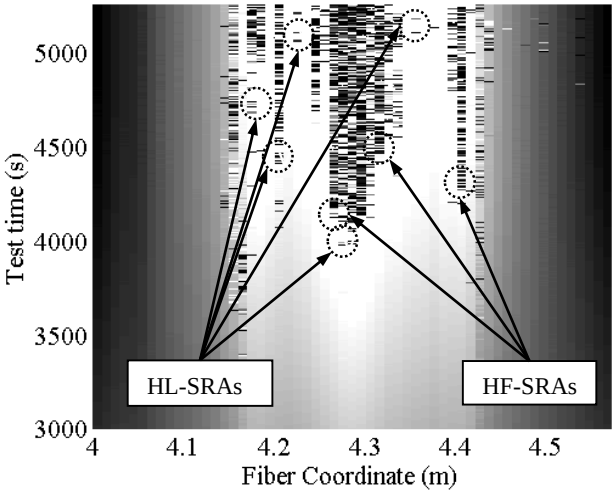

Figure 9. Two dimensional representation of DOFS-measured strains along time over the span of the fiber bonded to the Bar 5 and example of distinction between harmless and harmful SRAs

A quick glance of (Fig. 9) shows the existence of some SRAs which, despite preventing the correct reading of the strains in that particular fiber coordinate/s and instances, allows it further on in the test. Other SRAs instead are followed by further anomalies for all the remaining duration of the test making impossible to extract any further reliable strain readings. It is worth distinguishing the two as one represents the end of any reliable strain measurements in a specific section Harmful Anomalies (HF-SRA), while the others do not and are therefore defined as Harmless Anomalies (HL-SRA). (Fig. 10) plots, for every section of the rebars, the strain values at which the first HL-SRA and HF-SRA spring up therefore giving a graphical representation of the SRAs relation with strains.

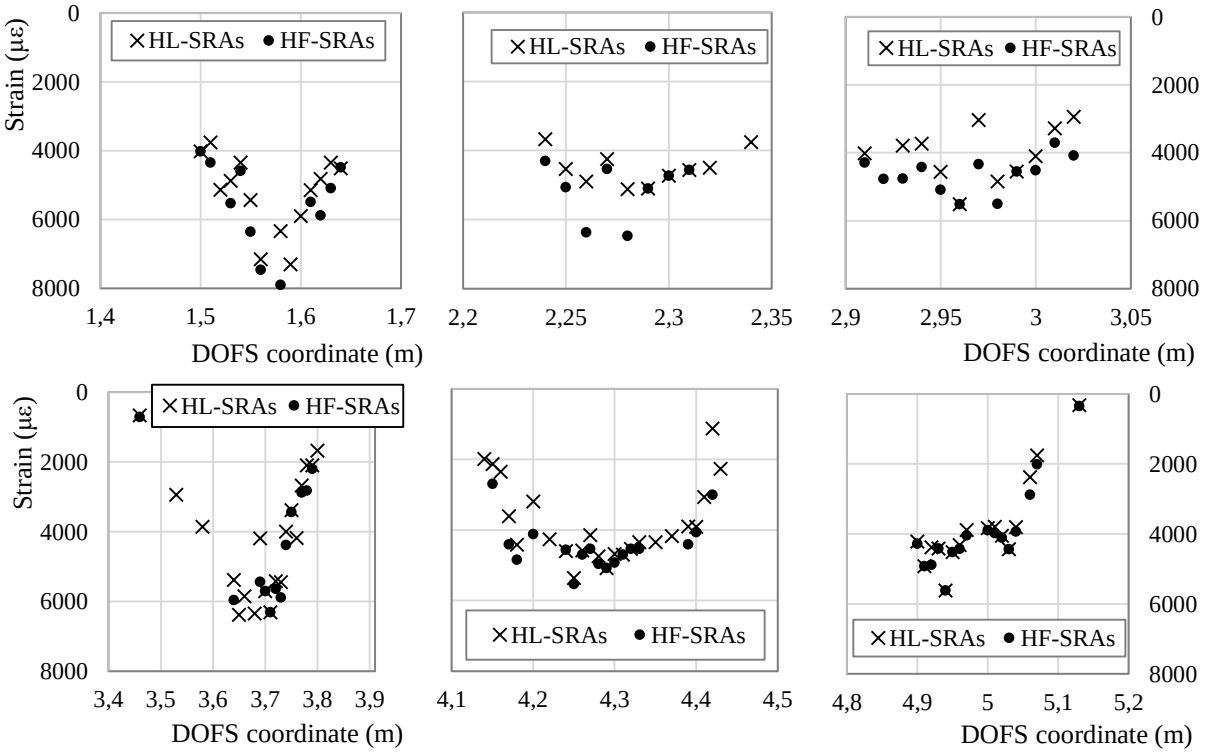

Figure 10. Plotting of DOFS-measured strain values at which the first HL-SRA and HF-SRA are recorded in each DOFS coordinate with anomalies

Some interesting observations can be developed based on (Fig. 8-10):

- Except for a few DOFS sections, the SRAs start beyond the specimen´s plasticity point reached around 3800 seconds (around 4000με).
- SRAs are often concentrated in specific areas where all neighboring sections give evidence of anomalistic behavior. Such areas can be defined as Anomalistic areas.
- Averagely SRAs seem to spring up from the mid-span of the rebars first which, not coincidentally, are the most stressed points of the seven rebars. The anomalies later spread outwards towards the neighboring section, as evident in Bars 2, 3, 6, forming an anomalistic area (Fig. 8).
- In Bars 4, 5, 6, the SRAs also rise in the incised sections concurrently or soon after having appeared in the mid-span (particularly evident in Bar 5). This further confirms the hypothesis of SRAs springing up from highly stressed rebar sections.
- HF-SRAs are usually proceeded by HL-SRAs.
- In some rebars HL-SRAs seem to start slightly before the specimen´s plasticity point whilst all HF-SRAs after. In particular Bar 3 starts having HL-SRAs as soon as 3000 seconds at section 2.97m.
- In some cases, a DOFS section can be characterized strictly by HL-SRAs guaranteeing intervals of strain readability such as DOFS coordinate 4.15m in bonded to Bar 4 (Fig .7).

As evident from (Fig. 9) and (Fig. 10), on the edges of the anomalistic areas, the SRAs spring up at lower and lower strains the more their sections are distant from the mid-span of the rebar (much lower than the hypothized AST). This could debunk the possibility of the existence of an AST. On the other hand, it can still be plausible considering the presence of the following phenomena. Assuming the existence of an influence that a section's anomalistic behavior has on neighboring ones causing them to also have SRAs, then it would be sufficient that the mid-span of a rebar suffered of the first SRA to start a chain reaction leading to the creation of the anomalistic area. This would prevent the sections involved in such area to reach the AST triggering the SRA prematurely. Another point in favor of the existence of an AST is suggested by the location of most HF-SRAs in (Fig .10). Indeed, 83% of HF-SRAs are triggered at a strain level beyond 4000με whilst the other 17% are HF-SRAs that have sprung up on the edges of anomalistic areas. The smaller portion of HF-SRAs are probably triggered prematurely by the above described effect.

In conclusion the SRAs seem to proliferate on all six DOFS instrumented bars in the most stressed sections (mid-span or/and incisions). Such phenomenon occurred in both full and incised sections and at a much later instance than the application of two impact loads. As a consequence, DM-SB2 (for small impact loads) and DM-SB3 can be discarded as potential triggers of the SRAs. Harmless anomalies (HL-SRAs) rise earlier than Harmful ones (HF-SRAs) but, being the proliferation of the latter more troublesome in experimental tests, they are the focus for the determination of an anomalistic strain threshold AST of 4000με (DM-SB1). The latter coincides time-wise (3800 seconds) with the specimen's change in deformative behavior and deviation from its previously linear load-displacement graph. The coincidence of these two phenomena prevents the pin-pointing of which of the two is the trigger of the SRAs. Further experimental investigation is therefore required.

On the disruption mechanism DM-AD1, the absence of concrete in the test prevented from checking the role that the friction of cracking concrete has in the rise of SRAs. Meanwhile for DM-AD2 and DM-AD3 no apparent debonding was evident while only a small crack in cyanoacrylate was spotted. Yet, no anomalistic correlation can be found in the cracked section suggesting that only the most superficial layer of the adhesive has cracked, leaving intact the one below in direct contact with the DOFS. As a consequence of such, assuming a correct positioning of the adhesive these two disruption mechanisms can be discarded from the possible causes for the rise of SRAs. Finally, reliable measurements were taken both with cyanoacrylate and silicone until high strain levels, removing DM-AD4 from the possible causes of the rise of SRAs.

3. Conclusions

The experimental test demonstrated once again the large potential of DOFS for strain measurements on/inside civil engineering structures. The strains measured were indeed congruent both with the structure's expected theoretical response and with the strains measured in parallel by the strain gauges. This, at stress levels of both small and large entity (more than double of the yielding stress) and in a completely distributed manner. The Strain Reading Anomalies, above defined as SRAs, were triggered beyond a rather clear threshold while their possible causes were isolated. Indeed, of the seven possible causes for the rise of SRAs, named Disruption Mechanisms (DM), the only ones that weren't excluded by the present test are the following:

- (DM-SB1) The existence of a Strain Anomaly Threshold (AST) beyond which the constitutive material of the fiber can't bear any more stresses without showing anomalies in the readings was only partially confirmed. On the other hand, when the fibers are already under stress they may suffer a sensibility to variations in the mechanical behavior of its support.
- (DM-SB2) The present test was designed in such a way that only minor impact loads could be applied. Therefore, in order to correctly simulate the peaking of stresses that rebars experience whenever a crack opens in a specific section, further experimentation is required with higher impact loads or actual cracking concrete.
- (DM-AD1) The absence of concrete in the test prevented the checking of the role that the friction of cracking concrete has in the rise of SRAs.

An experimental campaign will follow up the present one by studying the influence of the remaining disruption mechanisms on RC tie members. Yet, the current experiment helped shedding light on the anomalistic behavior of DOFS. The following conclusions were extrapolated:

- The SRAs tend to rise in multiple neighboring DOFS sections forming Anomalistic areas.
- The anomalistic areas focus around sections of the rebar that are heavily stressed (such as the mid-span and the incised sections).
- The SRAs can be distinguished between Harmless SRAs (HL-SRAs) and Harmful SRAs (HM-SRAs) of which only the latter represents a serious threat for the research. Indeed, in the case of the first type of anomalies, following some anomalistic measurements are multiple reliable ones making the HL-SRAs more of a nuisance than limit.
- Even though some HL-SRAs seem to appear earlier, most SRAs and all the HF-SRAs occur beyond a specific moment in the test which sees simultaneously the reaching of the strain value of roughly 4000με (possible AST) in all the bars of the specimen and the yielding of the fixed ends of the bars which caused a variation in the specimen's load-deformation behavior. One or both these elements seem to have triggered the rise of SRAs.
- The adhesives used to bond the DOFS to their support didn't cause the rise of SRAs.

References

[1] A. Barrias, J. Casas, and S. Villalba, "A Review of Distributed Optical Fiber Sensors for Civil Engineering Applications," *Sensors*, vol. 16, no. 5, p. 748, 2016.

[2] B. Glišić, D. Hubbell, D. H. Sigurdardottir, and Y. Yao, "Damage detection and characterization using long-gauge and distributed fiber optic sensors," *Opt. Eng.*, vol. 52, no. 8, p. 087101, 2013.

[3] P. Ferdinand, "The Evolution of Optical Fiber Sensors Technologies During the 35 Last Years and Their Applications in Structure Health Monitoring," *EWSHM-7th Eur. Work. Struct. Heal. Monit.*, 2014.

[4] A. Deif, B. Martín-Pérez, B. Cousin, C. Zhang, X. Bao, and W. Li, "Detection of cracks in a reinforced concrete beam using distributed Brillouin fibre sensors," *Smart Mater. Struct.*, vol.

19, no. 5, 2010.
[5] X. Bao and L. Chen, “Recent Progress in Distributed Fiber Optic Sensors,” *Sensors*, vol. 12, no. 12, pp. 8601–8639, 2012.
[6] A. Barrias, J. Casas, and S. Villalba, “Embedded Distributed Optical Fiber Sensors in Reinforced Concrete Structures—A Case Study,” *Sensors*, vol. 18, no. 4, p. 980, 2018.
[7] S. Villalba and J. R. Casas, “Application of optical fiber distributed sensing to health monitoring of concrete structures,” *Mech. Syst. Signal Process.*, vol. 39, no. 1–2, pp. 441–451, 2013.
[8] R. M. Measures, “Structural Monitoring with Fibre Optic Technology,” *Meas. Sci. Technol. - MEAS SCI TECHNOL*, vol. 12, pp. 1609–1610.
[9] A. Barrias, J. R. Casas, and S. Villalba, “Application study of embedded Rayleigh based Distributed Optical Fiber Sensors in concrete beams,” *Procedia Eng.*, vol. 199, no. 2017, pp. 2014–2019, 2017.
[10] M. Davis, N. A. Hoult, and A. Scott, “Distributed strain sensing to determine the impact of corrosion on bond performance in reinforced concrete,” *Constr. Build. Mater.*, vol. 114, pp. 481–491, 2016.
[11] M. Davis, N. A. Hoult, and A. Scott, “Distributed strain sensing to assess corroded RC beams,” *Eng. Struct.*, vol. 140, pp. 473–482, 2017.
[12] B. Andre, N. Sara, and N. A. Hoult, “Distributed Deflection Measurement of Reinforced Concrete Elements Using Fibre Optic Sensors,” in *Proceedings of the International Association for Bridge and Structural Engineering (IABSE) Symposium*, pp. 1469–1477.
[13] G. Kaklauskas, “Crack Model for RC Members Based on Compatibility of Stress-Transfer and Mean-Strain Approaches,” vol. 143, no. 9, pp. 1–12, 2017.